Journal of Organometallic Chemistry 694 (2009) 3511–3517

Contents lists available at ScienceDirect

Journal of Organometallic Chemistry

journal homepage: www.elsevier.com/locate/jorganchem

Design and synthesis of 2-substituted-8-hydroxyquinline zinc complexes with hole-transporting ability for highly effective yellow-light emitters

Xinhua Ouyang [a], Guangrong Wang [a], Heping Zeng [a,b,*], Weiming Zhang [a], Jing Li [a,c,*]

[a] Institute of Functional Molecule, South China University of Technology, Guangzhou 510641, People's Republic of China
[b] School of Chemistry and Environment, South China Normal University, Guangzhou 510631, People's Republic of China
[c] Department of Chemistry and Chemical Biology, Rutgers University, 610 Taylor Road, Piscataway, NJ 08854, USA

ARTICLE INFO

Article history:
Received 20 May 2009
Received in revised form 15 June 2009
Accepted 18 June 2009
Available online 23 June 2009

Keywords:
2-Substituted-8-hydroxyquinolate-zinc
Yellow-light emitting material
Multifunctional material

ABSTRACT

Four multifunctional 8-hydroxyquinoline derivatives were designed and synthesized, their structures were identified by FT-IR, ^{1}H NMR, MS and elemental analysis. Among them are (*E*)-2-(2-(9-(4-methoxyphenyl)-9H-carbazol-3-yl)vinyl) quinolato-zinc (**1**), (*E*)-2-(2-(9-p-tolyl-9H-carbazol-3-yl)vinyl)quinolato-zinc (**2**), (*E*)-2-(2-(9H-fluoren-2-yl)vinyl)quinolato-zinc (**3**), and (*E*)-2-(2-(phenanthren-9-yl)vinyl)quinolato-zinc (**4**). The electroluminescence (EL) and hole-transporting characteristics of these materials were investigated on four configurations: (A) ITO/2-TNATA/NPB/1, 2, 3 or 4/Alq_3/LiF/Al; (B) ITO/2-TNATA/NPB/1, 2, 3 or 4/LiF/Al; (C) ITO/2-TNATA/1, 2, 3 or 4/Alq_3/LiF/Al; and (D) ITO/2-TNATA/1 or 2/NPB/Alq_3/LiF/Al. The maximum luminescence and current efficiencies of are 3556 cd m^{-2} (at 13 V) and 2.17 cd A^{-1} (at 9 V) for compound **2**, 4624 cd m^{-2} (at 15 V) and 2.1 cd A^{-1} (at 7 V) for compound **3**, and 3164 cd m^{-2} (at 14 V) and 1.83 cd A^{-1} (at 13 V) for compound **4** in the configuration D, respectively, indicating that they are good multifunctional materials with strong hole-transporting abilities and luminescence properties.

1. Introduction

Organic photo- and electronic materials have commanded increasing attention since the discovery of organic conductors [1–3], which offer large-area, flexible, and lightweight devices through simple and low-cost processing. During the past twenty years, much effort has been paid to the development of highly efficient organic light-emitting diodes (OLEDs) [4–6], especially the white OLEDs [7–10]. To obtain white emission, various strategies have been developed. For small-molecule OLEDs, the general approach is to fabricate multiplayer devices by consecutive evaporation involving three primary colors (blue, green and red) or two special colors (blue and yellow). However, multiplayer construction of devices will increase of the cost of fabrication processes. In order to reduce the cost and obtain white OLEDs with minimal process of fabrication, it would be necessary to discover multifunction and highly efficient yellow-light emitting materials.

8-Hydroxyquinoline aluminum (Alq_3) has been identified as an excellent green-light emitting and electronic transporting material [11]. In order to retain the excellent photoelectron properties of 8-hydroxyquinoline itself and achieve yellow-light emission, a feasible approach is to extend the degree of π-conjugation in 8-hydroxyquinoline molecule, which will bring about a huge bathochromic effect. Meanwhile, some OLEDs with highly electroluminescent efficiencies can be also obtained by modifying the quinoline ring with differently functional groups. Active research in this area has been conducted over the past twenty years. For example, Mishra et al. [12] synthesized several 5-alkoxymethyl- and 5-aminomethy substituted 8-hydroxyquinoline alumina complexes, which were characteristic of strong green-light emissions with high quantum yields. Cui et al. [13] also reported 2-substitued-8-hydroxyquinoline molecules with large conjugated groups and tuned their luminescence to yellow-light (λ_{ex} = 610 nm). Likewise, Xie et al. [14] synthesized a new 5-substitued-8-hydroxyl quinoline exhibiting bi-functional and dipolar behavior. Their results showed that this molecule can be used as hole and electron transporter and emitter. Therefore, the incorporation of electron-donors (chemical structure suitable for capturing hole carriers) and electron-acceptors (chemical structure suitable for capturing electron carriers) into one molecule is highly desirable to enhance performance and improve fabrication technology.

In this paper, we report the synthesis, device fabrication and electroluminescence measurements of 2-substituted-8-hydroxy-quinolato-Zn derivatives containing two different carbazole, fluorine and phenanthrene units owing to their abilities in luminescence and charge-transfer [15–18]. These four compounds

* Corresponding authors. Address: Institute of Functional Molecule, South China University of Technology, Guangzhou 510641, People's Republic of China.
E-mail addresses: hpzeng@scut.edu.cn (H. Zeng), jingli@rutgers.edu (J. Li).

0022-328X/$ - see front matter © 2009 Elsevier B.V. All rights reserved.
doi:10.1016/j.jorganchem.2009.06.022

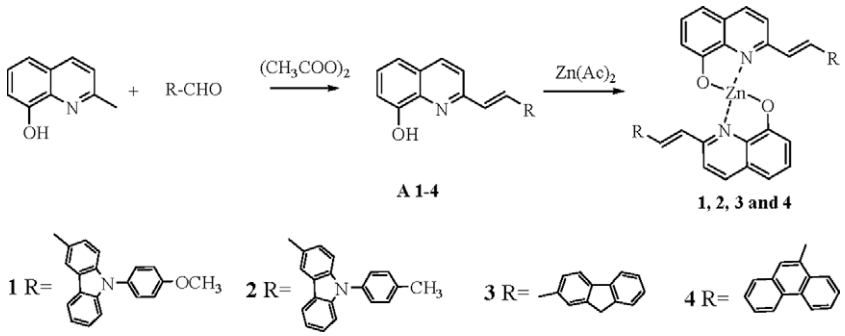

Scheme 1.

are: (*E*)-2-(2-(9-(4-methoxyphenyl)-9H-carbazol-3-yl)vinyl)quinolato-zinc (**1**), (*E*)-2-(2-(9-p-tolyl-9H-carbazol-3-yl)vinyl)quinolato-zinc (**2**), (*E*)-2-(2-(9H-fluoren-2-yl)vinyl)quinolato-zinc (**3**) and (*E*)-2-(2-(phenanthren-9-yl)vinyl)quinolato-zinc (**4**). The synthetic route of **1**, **2, 3** and **4** is shown in Scheme 1. In combination of 8-hydroxyquinoline with fluorene and carbazole, we anticipate the formation of new dipolar and multifunctional materials with excellent performance. Optical, thermal properties of these compounds were investigated, and electroluminescent devices using them as emission layers (EL), hole-transporting layers (HTL) or EL&HTL were fabricated and characterized.

2. Results and discussions

The thermal properties of the 8-hydroxyquinoline derivatives, investigated by differential scanning calorimetry (DSC) and thermo-gravimetric analysis (TGA), are summarized in Table 1. The glass-transition temperatures (T_gs) of all four compounds are around 181–187 °C. **3** exhibits the highest T_g (187 °C), due to its rigid fluorene structure segment. Thermal decomposition temperatures (T_ds) of all compounds are around 360–480 °C. The results indicate that the incorporation of π-conjugated bridges into the 8-hydroxyquninoline system enhances the thermal properties significantly, especially with the fluorene derivative comparing with the publications about 2-methyl-8-hydroxylquinolato-zinc (T_g, 103 °C) [19].

The absorption data for the four compounds are also summarized in Table 1 and Fig. 1a. Among the four compounds, the maximal absorptive peaks of **1** and **2** are very similar and centered at about 380 nm, and the absorption spectra of **3** and **4** are also almost identical and at a maximum wavelength of ~350 nm, due to their similar π-conjugation structures and lengths. In the meanwhile, we also plotted the absorptive spectra of **A1**–**A4** in Fig. 1a, it can be seen the spectra appeared clear difference between the samples **A1**–**A4** and samples 1–4, which indicated there were interactions among them. The phenomena can be attributed to charge-transfer form metal-to-ligand transitions (MLCT) or ligand-to-metal transitions (LMCT). Photoluminescence (PL) data for these samples in solution and in solid state are recorded in Table 1 and Fig. 1b. The PL emissions of the four compounds appear around 567–585 nm in solution state and 591–628 nm in solid state. The spectra obtained for the solid state are red-shifted in relation to the solution measurements, as can be seen in Table 1, due to the molecular aggregation. Molecular aggregation leads to shifts of the state energies depending on the mutual orientation of the molecules forming a dimer, different transitions in the system can be forbidden or allowed. The optical properties associated with H-aggregates and J-aggregates [20]. It has been shown that H-type molecular aggregates result in the shift of the luminescence band. The insertion of π-conjugation bridging moieties also causes a significant red-shift in the spectra: **1**, **2**, **3** and **4** exhibit yellow to orange-red emission at peak wavelengths (λ_{max}^{PL}) at 591, 593, 602 and 628 nm, respectively. Thus, the photophysical properties of these emitters are strongly affected by the π-conjugation lengths. Similar to the absorption spectra, the PL spectrum of **4** is red-shifted

Table 1
Summary of physical properties of compounds **1, 2, 3** and **4**.

	λ_{max}^{abs} (nm)	λ_{max}^{em} (nm) in DMF	λ_{max}^{em} (nm) in solid	Φ	T_g (°C)	T_d (°C)	τ (ns)
1	382	576	591	0.096	184	372	3.23
2	383	571	593	0.094	186	381	3.34
3	351	585	602	0.076	187	363	3.58
4	345	567	628	0.08	181	382	3.42

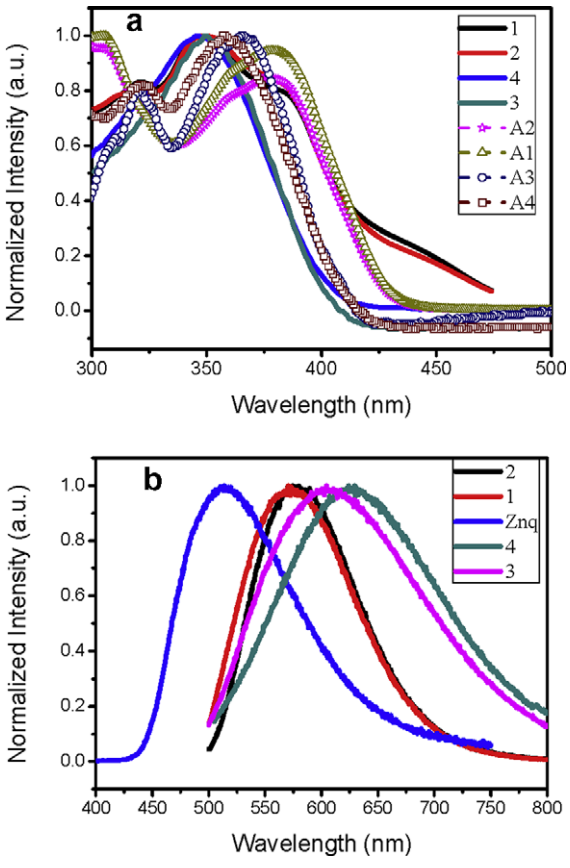

Fig. 1. (a) The absorptive spectra of samples 1, 2, 3 and 4 in DMF; (b) the PL spectra of samples 1, 2, 3, 4 and Znq in solid states.

to 628 nm, compared with 515 nm for 8-hydroxy-quinolato-Zn (Znq), because of the electron-rich nature of phenanthrene ring and its lower aromaticity relative to that of a benzene ring.

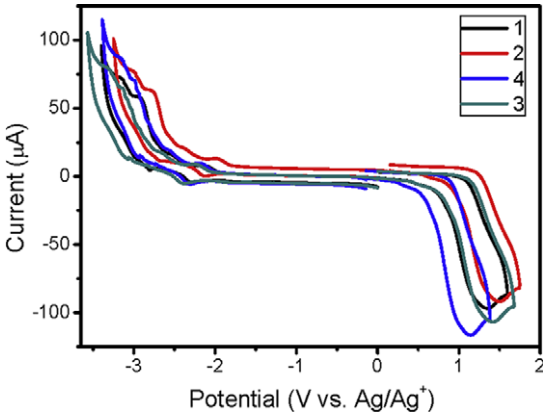

Fig. 2. Cyclic voltammograms of **1**, **2**, **3**, and **4** with the concentration of 0.001 M in 0.1 M Bu_4NPF_6-DMF, with a glassy carbon electrode at a scan rate of 50 mV s^{-1}. A platinum wire and an Ag/AgCl were used as the counter and reference electrode, respectively.

Table 2
Electrochemical parameters of compounds **1**, **2**, **3** and **4**.

Compounds	E^{red}_{onset} (V)	E^{ox}_{onset} (V)	E_g (eV)[a]	HOMO (eV)	LUMO (eV)
1	−1.96	0.39	2.16	−5.19	−3.03
2	−1.81	0.56	2.18	−5.36	−3.18
3	−2.05	0.38	2.12	−5.18	−3.06
4	−2.01	0.22	2.19	−5.02	−3.01

[a] E_g estimated from maximal emission peak energy.

3. Electrochemical properties

Cyclic voltammetry (CV) was employed to investigate the electrochemical behaviors of the compounds **1**, **2**, 3 and **4**. The highest occupied molecular orbital (HOMO) and lowest unoccupied molecular orbital (LUMO) energy levels of the materials were estimated according to the electrochemical performance and emission spectra. Oxidation behaviors of **1**, **2**, **3**, and **4** have been investigated in DMF as shown in Fig. 2, and the results are summarized in Table 2. The HOMO energy values for these compounds were calculated based on the value of −4.8 eV for ferrocene with respect to zero vacuum level.

In order to assess their electroluminescence functionality, each of the four compounds was fabricated into four different device structures. The device structures and related information are outlined in Fig. 3. In these configurations of A, B, C and D, ITO glass is used as transparent anode, *N*-(naphthalene-2-yl)-*N*′,*N*′-bis(naphthalene-2-yl(phenyl)amino)phenyl)-*N*-phenylbenzene-1,4-diamine(2-TNATA) is used as hole-injecting material (HIM), due to its energy of the highest occupied orbit (HOMO), which is close to the energy of HOMO of ITO (4.8 eV), tris-8-hydroxyl-quinolato-aluminum (Alq_3) as electron-transporting material (ETM) and lithium fluoride (LiF) as the buffer layer, due to its energy of the lowest unoccupied orbit (LUMO), which is close to the energy of LUMO of Al (3.7 eV). Samples of compounds **1**, **2**, **3** and **4** acted as emitter in configuration A, emitter and ETM in configuration B, emitter and hole-transporting materials (HTM) in configuration C, and HTM and ETM in configuration D, respectively, for which luminescence, HT and ET properties were examined. *N*,*N*′-bis(naphthyl)-*N*,*N*′-diphenyl-1,1′-biphenyl-4,4′-diamine (NPB) was used as HTM in the configuration A and B, and emitter in the configuration D.

The normalized EL spectra of compounds **1**, **2**, **3** and **4** in devices A, B and C at 14 V are shown in Fig. 4. The EL spectra of **1**, **3** and **4** are very similar in these configurations. It is obvious that they

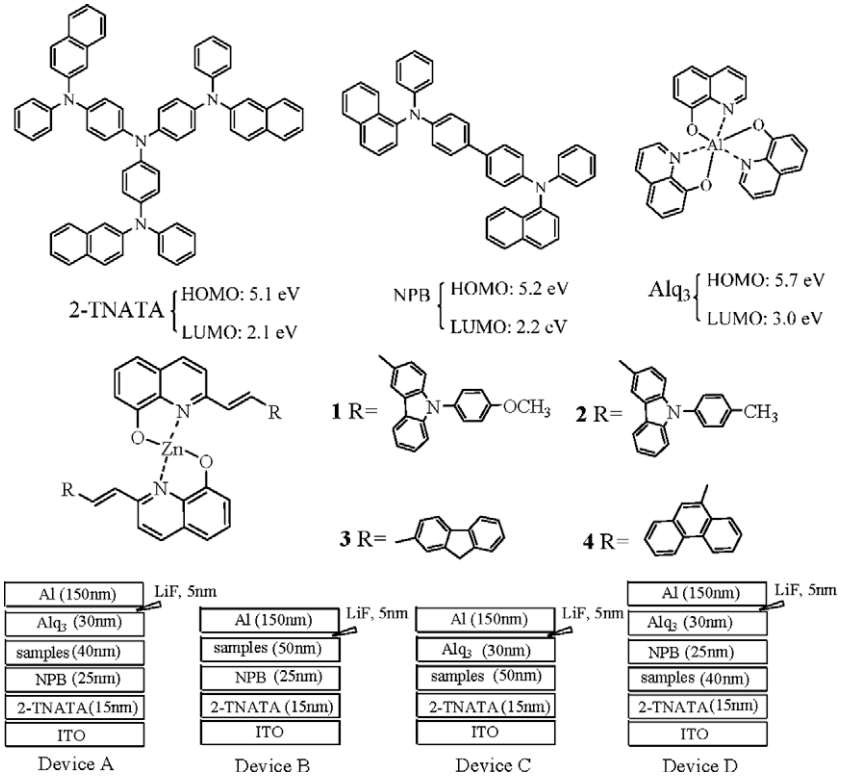

Fig. 3. The molecular structures of organic materials and the device structures of the OLEDs.

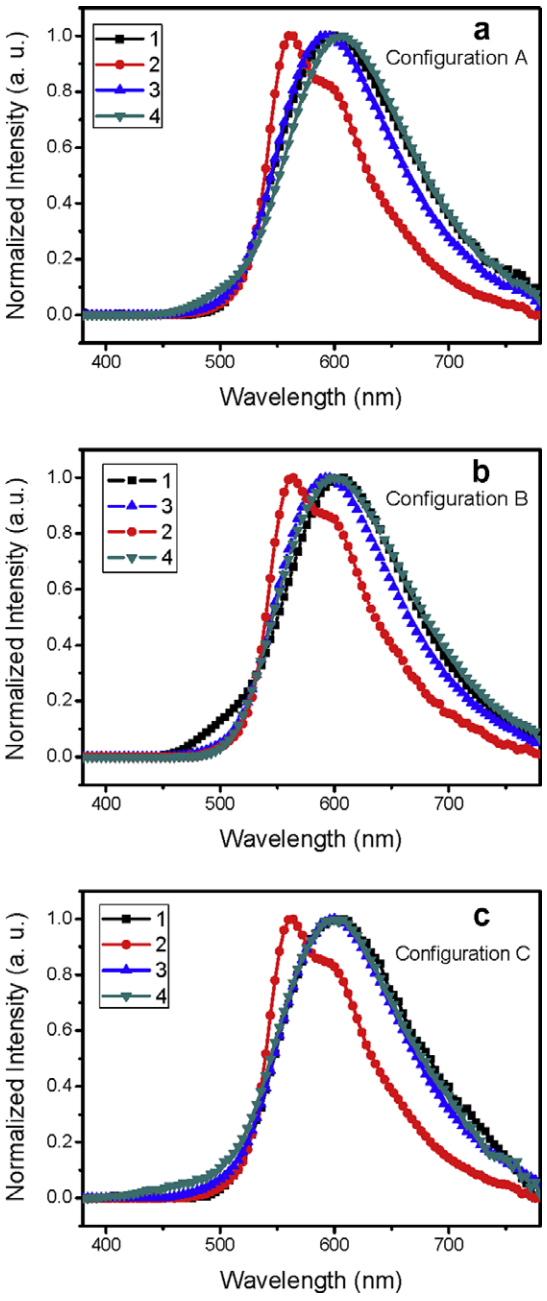

Fig. 4. The EL spectra of **1**–**4** in (a) device A; (b) device B; and (c) device C.

exhibit yellow-light emission. Further analysis showed that all compounds act as the emitter in the devices A–C. The results also clearly indicate that the observed yellow emission originates from the compounds **1**, **2**, **3** and **4** layers by comparing electroluminescence with photoluminescence spectra. Some of important parameters of these devices are given in Table 3. CIE coordinates of the three different devices with compounds **1**, **2**, **3** and **4** as a function of applied voltages.

Luminescent brightness–voltage (*L*–*V*) and current efficiency–voltage (*E*–*V*) characteristics of devices A–C are shown in Figs. 5 and 6, respectively. In device A, NPB acted as a hole-transporting (HTL), Alq_3 as an electron-transporting layer (ETL), and samples of **1**, **2**, **3** and **4** as yellow-light emitting layers. Maximum luminance brightness of device A for **1**, **2**, **3** and **4** are 1420 cd m^{-2} (at 14 V), 3596 cd m^{-2} (at 14 V), 2782 cd m^{-2} (at 14 V), and 2654 cd m^{-2} (at 14 V), respectively, and the maximum luminescent efficiencies for **1**, **2**, **3** and **4** are 0.67 cd A^{-1} (at 10 V), 1.76 cd A^{-1} (at 9 V), 1.08 cd A^{-1} (at 13 V), and 0.89 cd A^{-1} (at 13 V), respectively. In device B, one can easily find that the Alq_3 is removed in order to investigate the electron-transporting properties and luminescent properties of **1**, **2**, **3** and **4**. The maximum luminescent brightness and maximum current efficiencies of device B for **1**, **2**, **3** and **4** are 697 cd m^{-2} (at 15 V) and 0.31 cd A^{-1} (at 14 V), 192 cd m^{-2} (at 13 V) and 0.15 cd A^{-1} (at 13 V), 1222 cd m^{-2} (at 10 V) and 0.35 cd A^{-1} (at 9 V), and 379 cd m^{-2} (at 15 V) and 0.78 cd A^{-1} (at 13 V), respectively. In the device C, we removed the hole-transporting layer (NPB) in comparison with the structure of device A, and the maximum luminescent brightness and current efficiencies for samples of **1**, **2**, **3** and **4** are 1396 cd m^{-2} (at 14 V) and 0.96 cd A^{-1} (at 13 V), 3596 cd m^{-2} (at 14 V) and 1.76 cd A^{-1} (at 9 V), 3384 cd m^{-2} (at 10 V) and 0.92 cd A^{-1} (at 9 V), and 3531 cd m^{-2} (at 14 V) and 0.79 cd A^{-1} (at 12 V). By comparing the maximum luminescence and current efficiencies in all of the devices, we noted that **1** is not good as yellow-light emitter, ELM and HLM materials due to its low luminescence and efficiencies, and compound **3** is a good candidate as multifunctional material such as emitter, ELM and HLM. Likewise, the compounds **2** and **4** can be use as dipolar materials such emitters and HLMs. Comparing the results with the publication of literature [21], we can find the maximum luminescent brightness of published sample was 1200 cd m^{-2} using undoped yellow emitter, which indicated our results improved significantly the yellow luminescent brightness. It will provide a new method to enhance the yellow brightness.

In order to investigate in further depth the multifunctional properties of **2**, **3** and **4**, we designed another configuration D (Fig. 3) to test the Hole-transporting and luminescence properties. The samples of **2**, **3** and **4** were used as HTM and yellow-light emitters and the results are summarized in Fig. 7. By analyzing

Table 3
The results of compounds **1**, **2** and **3** in the devices A, B and C.

Device (samples)	$Luminance_{max}$ (cd m^{-2})	CIE coordinates (*x*, *y*) ($luminance_{max}$)	EL $efficiency_{max}$ (cd A^{-1})	CIE coordinates (*x*, *y*) ($efficiency_{max}$)	Turn-on voltage (V)	Power efficiency η_{Pmax} (lm/w)
A (1)	1420 @ 14 V	(0.5283, 0.4642)	0.67 @ 10 V	(0.5351, 0.4593)	8	1.25
A (2)	3596 @ 14 V	(0.4915, 0.4954)	1.76 @ 9 V	(0.4979, 0.4946)	4	3.3
A (3)	2782 @ 14 V	(0.5189, 0.4691)	1.08 @ 13 V	(0.5189, 0.4691)	5	1.03
A (4)	2654 @ 14 V	(0.5253, 0.4483)	0.89 @ 13 V	(0.523, 0.4499)	6	1.91
B (1)	697 @ 15 V	(0.518, 0.4701)	0.31 @ 14 V	(0.5259, 0.4657)	7	0.6
B (2)	192 @ 13 V	(0.5, 0.4924)	0.15 @ 13 V	(0.5, 0.4924)	5	0.0
B (3)	1222 @ 10 V	(0.5205, 0.4713)	0.35 @ 9 V	(0.5294, 0.4647)	6	0.55
B (4)	379 @ 15 V	(0.5343, 0.4446)	0.78 @ 13 V	(0.5337, 0.4526)	5	0.0
C (1)	1396 @ 14 V	(0.529, 0.4633)	0.96 @13 V	(0.5311, 0.4622)	7	1.92
C (2)	3596 @ 14 V	(0.4915, 0.4954)	1.76 @ 9 V	(0.4979, 0.4946)	6	4.
C (3)	3384 @ 10 V	(0.5271, 0.459)	0.92 @ 9 V	(0.5317, 0.4564)	8	1.22
C (4)	3531 @ 14 V	(0.5474, 0.4435)	0.79 @ 12 V	(0.5353, 0.4435)	6	3.1

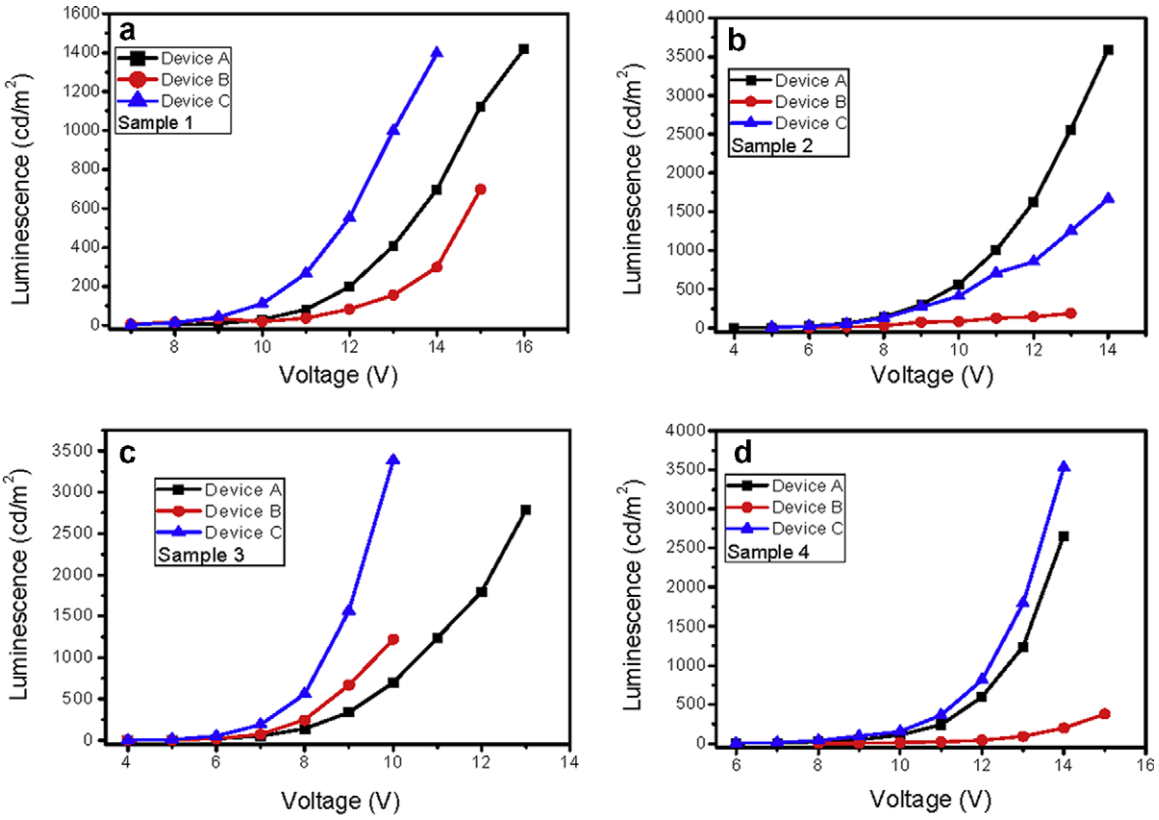

Fig. 5. The voltage–luminescence curves of samples of 1, 2, 3 and 4 in devices A, B and C.

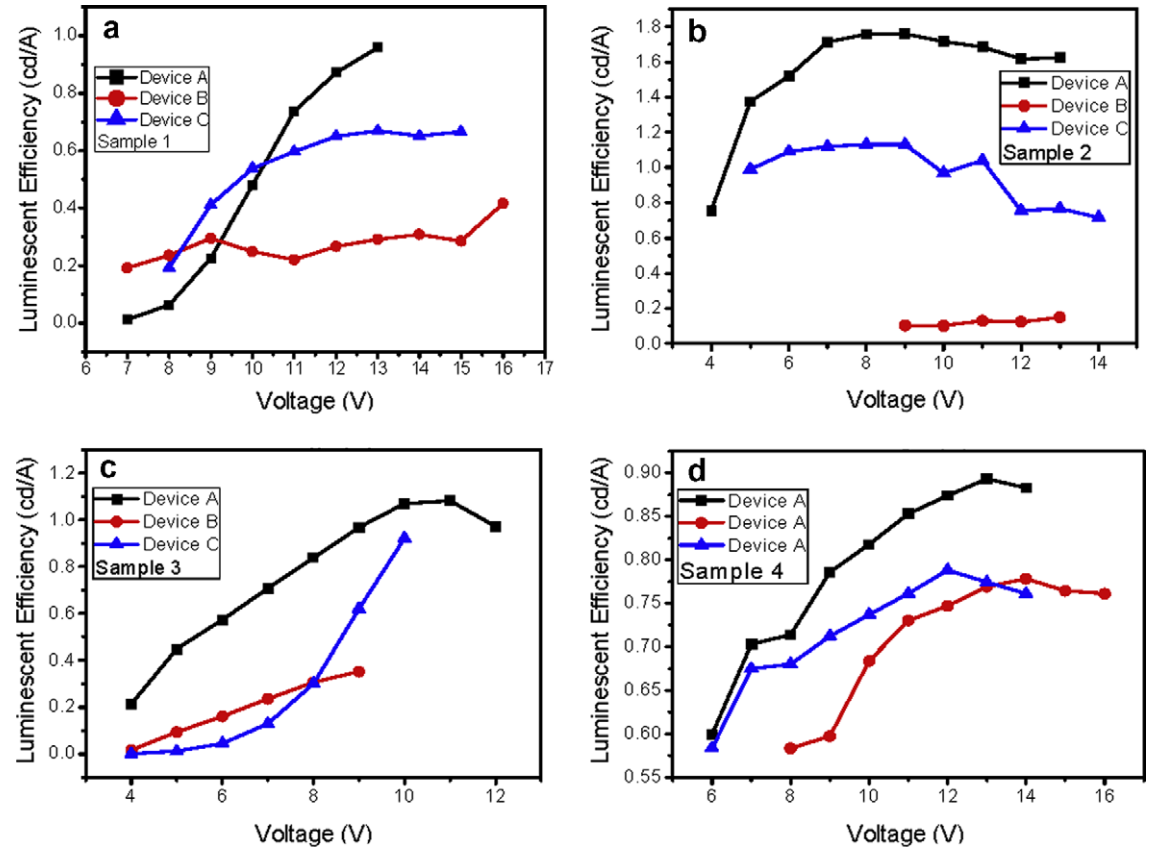

Fig. 6. The voltage–efficiency curves of samples of 1, 2, 3 and 4 in devices A, B, and C.

the results of device D, we find the luminescence of these samples is located at white-light range with two peaks in the EL spectra, one is from the samples, and another is from NPB. The maximum luminescence and efficiencies for **2**, **3** and **4** are 3556 cd m^{-2} (at 13 V) and 2.17 cd A^{-1} (at 9 V), 4624 cd m^{-2} (at 15 V) and 2.1 cd A^{-1} (at 7 V), and 3164 cd m^{-2} (at 14 V) and 1.83 cd A^{-1} (at 13 V), respectively. In this configuration, the efficiencies and brightness of the samples are improved significantly, demonstrating the good hole-transporting properties of **2**, **3** and **4**. In addition, they also show intensive luminescence in such a configuration. Further studies to optimize their performances by adjusting the thickness of yellow-light emitting layer (compounds **2**, **3** and **4**) and blue-light emitting layer (NPB) are currently under way.

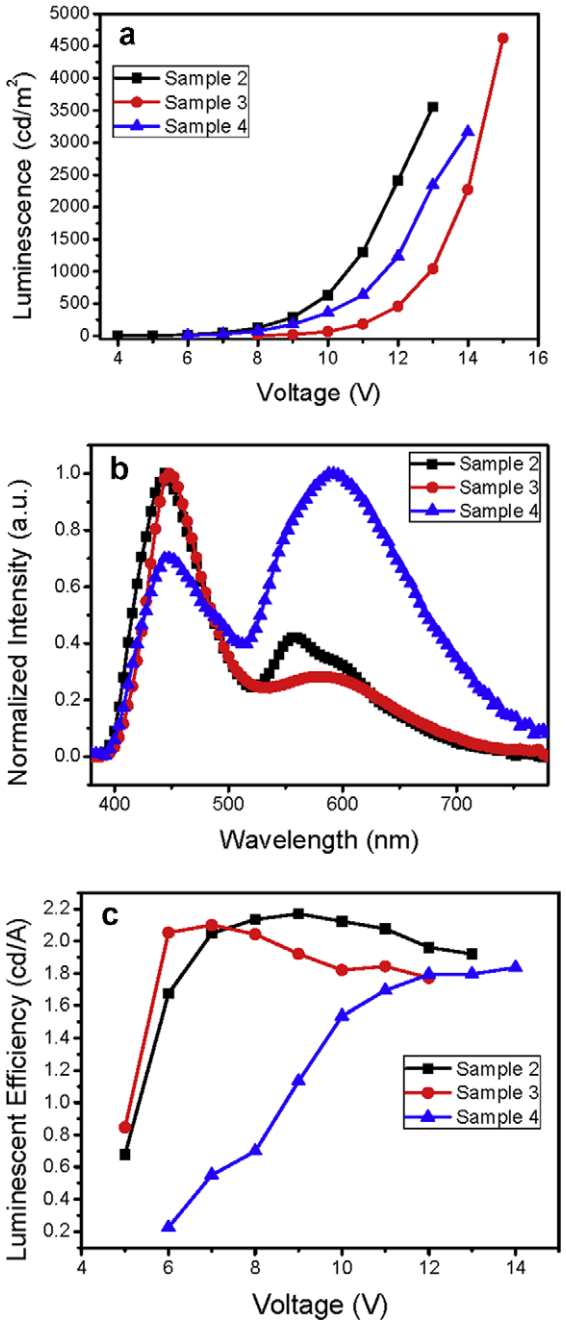

Fig. 7. The EL spectra, luminescence–voltage curves and efficiency–voltage curves for samples of 2, 3, and 4 in the device D.

4. Conclusions

We have synthesized four novel multifunctional 2-substituted-8-hydroxyquinline zinc complexes and their structures have been analyzed by FT-IR, ^{1}H NMR, MS and element analysis. The electroluminescence (EL) and hole-transporting characteristics of these bi-functional emitting materials have been studied by designing four device configurations. In device A, the maximum luminescence for **1**, **2**, **3** and **4** are 1420 cd m^{-2} (at 14 V), 3596 cd m^{-2} (at 14 V), 2782 cd m^{-2} (at 14 V), and 2654 cd m^{-2} (at 14 V), respectively, and the maximum luminescent efficiencies for **1, 2, 3** and **4** are 0.67 cd A^{-1} (at 10 V), 1.76 cd A^{-1} (at 9 V), 1.08 cd A^{-1} (at 13 V), and 0.89 cd A^{-1} (at 13 V), respectively. In device B, the luminance and efficiencies for samples **1, 2, 3** and **4** are 697 cd m^{-2} (at 15 V) and 0.31 cd A^{-1} (at 14 V), 192 cd m^{-2} (at 13 V) and 0.15 cd A^{-1} (at 13 V), 1222 cd m^{-2} (at 10 V) and 0.35 cd A^{-1} (at 9 V), and 379 cd m^{-2} (at 15 V) and 0.78 cd A^{-1} (at 13 V), respectively. In device C, these are 1396 cd m^{-2} (at 14 V) and 0.96 cd A^{-1} (at 13 V), 3596 cd m^{-2} (at 14 V) and 1.76 cd A^{-1} (at 9 V), 3384 cd m^{-2} (at 10 V) and 0.92 cd A^{-1} (at 9 V), and 3531 cd m^{-2} (at 14 V) and 0.79 cd A^{-1} (at 12 V). Our results show that **2, 3** and **4** are good multifunctional materials with strong hole-transporting abilities and luminescence properties.

5. Experimental

5.1. Materials

8-Hydroxy-2-methylquinoline, phenanthrene-9-carbaldehyde, and 9H-fluorene-2-carbaldehyde were purchased from Tokyo Chemical Industry Co., LTD. 9-*p*-Tolyl-9H-carbazole-3-carbaldehyde and 9-(4-methoxyphenyl)-9H-carbazole-3-carbaldehyde were synthesized according to the literatures [22,23]. $Zn(Ac)_2$, acetic anhydride and all solvents were obtained from Guangzhou chemical reagent company. The solvents were dried using standard procedures. All other reagents were used as received from commercial sources, unless otherwise stated.

5.2. Characterization

Melting points were determined using an Electro-thermal IA 900 apparatus and the thermometer was uncorrected. FT-IR spectra were recorded on a Perkin–Elmer Fourier transform infrared spectrometer and measured using KBr pellet. ^{1}H NMR spectra were determined in $CDCl_3$ with a Bruker DRX 400 MHz spectrometer. Chemical shifts (d) were given relative to tetramethylsilane (TMS). The coupling constants (*J*) were reported in Hz. Elemental analyses were recorded with a Perkin–Elmer 2400 analyzer. ESI-Ms spectra were performed with a FINNIGAN Trace DSQ mass spectrometer at 70 eV. Fluorescence emission spectra of these samples were measured with a FLSP920 spectrophotometer. Experiment was monitored by TLC. Column chromatography was carried out on silica gel.

5.3. General procedure for compound *A*

2-Methyl-8-hydroxyl-quinoline (2.0 mmol) and organic aldehydes (2.0 mmol) were dissolved in 10 ml of acetic anhydride. The mixture was stirred (magnetic stir bar) at 125 °C under a nitrogen atmosphere for 40 h and a brown precipitate was obtained. After cooling, the mixture was subsequently poured into 50 ml of ice-water and stirred overnight. The yellow solid obtained was filtered off and then purified by column chromatography on silica gel (200–300 mesh) using ethyl acetate/petroleum ether as eluant to give the product **A**.

A1: Yield, 61.2%; m.p. 147–148 °C; FT-IR (KBr) ν (cm^{-1}): 3386, 3030, 2951, 1624, 1589–1510, 1334, 1240; MS (ESI) *m*/*z*: 443 (M+H), ^1H NMR ($CDCl_3$, 400 MHz) δ: 3.86 (s, 3H), 7.32 (d, J = 7.6 Hz, 2H), 7.34 (d, J = 7.6 Hz, 1H), 7.37–7.40 (m, 2H), 7.41 (d, J = 7.4 Hz, 1H), 7.42–7.56 (m, 2H), 7.59 (d, J = 16.0 Hz, 1H) 7.80–7.82 (m, 2H), 7.83 (d, J = 7.8 Hz, 2H), 7.85 (d, J = 8.2 Hz, 1H), 8.16–8.20 (m, 2H), 7.30 (d, J = 16.0 Hz, 1H), 8.32 (d, J = 8.0 Hz, 1H), 10.40 (s, 1H). Anal. Calc. for $C_{30}H_{22}N_2O_2$: C, 81.43; H, 5.01; N, 6.33. Found: C, 81.52; H, 5.04; N, 6.27%.

A2: Yield, 62.5%; m.p. 149–150 °C; FT-IR (KBr) ν (cm^{-1}): 3389, 3029, 2954, 1645, 1593–1507, 1335; MS (ESI) *m*/*z*: 427 (M+H), ^1H NMR ($CDCl_3$, 400 MHz) δ: 2.36 (s, 3H), 7.10 (d, J = 7.6 Hz, 1H), 7.12–7.32 (m, 2H), 7.34 (d, J = 8.0 Hz, 2H), 7.38 (d, J = 7.4 Hz, 1H), 7.53–7.54 (m, 2H), 7.66 (d, J = 16.0 Hz, 1H), 7.70–7.79 (m, 2H), 7.93 (d, J = 7.8 Hz, 2H), 7.99 (d, J = 8.2 Hz, 1H), 8.02–8.10 (m, 2H), 8.28 (d, J = 16.0 Hz, 1H), 8.30 (d, J = 8.0 Hz, 1H), 10.02 (s, H). Anal. Calc. for $C_{30}H_{22}N_2O$: C, 84.48; H, 5.20; N, 6.57. Found: C, 84.61; H, 5.23; N, 6.51%.

A3: Yield, 41%; m.p. 164–166 °C; ^1H NMR ($CDCl_3$, 400 MHz) δ: 8.13 (d, J = 8.80 Hz, 1H), 7.79–7.85 (m, 4H), 7.67 (d, J = 8.80 Hz, 2H), 7.58 (d, J = 7.2 Hz, 1H), 7.38–7.48 (m, 3H), 7.28–7.36 (m, 2H), 7.18 (d, J = 6.4 Hz, 1H), 3.97 (s, 2H); FT-IR (KBr) ν (cm^{-1}): 3040, 1683, 1633, 1555, 960; MS (ESI) *m*/*z* (%): 337.4 (M+H). Anal. Calc. for $C_{24}H_{17}NO$: C, 85.94; N, 4.18; H, 5.11. Found: C, 85.90; N, 4.20; H, 5.15%.

A4: Yield, 0.30 g, 42%. m.p. 169–171 °C; ^1H NMR ($CDCl_3$, 400 MHz): δ 8.76 (d, J = 9.48 Hz, 1H), 8.68 (d, J = 8.80 Hz, 1H), 8.52 (d, J = 15.92 Hz, 1H), 8.31–8.33 (m, 1H), 7.28–7.36 (m, 2H), 8.17 (d, J = 8.50 Hz, 3H), 8.10 (s, 1H), 7.94 (d, J = 7.35 Hz, 1H), 7.61–7.75 (m, 5H), 7.40–7.50 (m, 2H), 7.32 (d, J = 7.29 Hz, 1H), 7.19 (d, J = 7.62 Hz, 1H); FT-IR (KBr) ν (cm^{-1}): 3048, 1687, 1630, 1562, 1458, 961; MS (ESI) *m*/*z* (%): 348.5 (M+H). Anal. Calc. for $C_{25}H_{17}NO$: C, 86.43; N, 4.03; H, 4.93. Found: C, 86.40; N, 4.03; H, 4.91%.

5.4. General Procedure for compounds **1, 2, 3** and **4**

Zn(II) complexes were prepared from **A1** to **A4** and zinc acetate dihydrate in DMF. Zinc acetate dihydrate (2.2 mmol, 0.413 g) was dissolved in 45 mL anhydrous methanol. The Zn(II) solution was added dropwise into the DMF (90 mL) solution of 1 mmol of **A** and kept stirring for 24 h. The yellow precipitate was filtered off, washed with methanol and dried in vacuum to afford **1**, **2**, **3** and **4**.

1: Yield, 68.9%; m.p. >300 °C; FT-IR (KBr) ν (cm^{-1}): 3025, 2954, 1648, 1592–1514, 1336, 1107, 515, 455; MS (FAB) *m*/*z*: 949 (M+H). Anal. Calc. for $ZnC_{60}H_{42}N_4O_4$: C, 75.92; H, 4.43; N, 5.90. Found: C, 76.03; H, 4.46; N, 5.87%.

2: Yield, 72.8%, m.p. >300 °C; FT-IR (KBr) ν (cm^{-1}): 3033, 2956, 1642, 1594–1513, 1337, 1104, 514, 458; MS (FAB) *m*/*z*: 915 (M+H). Anal. Calc. for $ZnC_{60}H_{42}N_4O_2$: C, 78.57; H, 4.58; N, 6.11. Found: C, 78.73; H, 4.60; N, 6.08%.

3: Yield, 91%; m.p. >300 °C; IR (KBr) ν (cm^{-1}): 3050, 2920, 2854, 1622, 1555, 1102, 520, 468; MS (FAB): 732.2 (M−H). Anal. Calc. for $ZnC_{48}H_{32}N_2O_2$: C, 78.58; N, 3.82; H, 4.37. Found: C, 78.43; N, 3.80; H, 4.33%.

4: Yield, 91%; m.p. >300 °C; IR (KBr) ν (cm^{-1}): 3050, 1622, 1555, 1102, 520, 468.06; MS (FAB): 757.9 (M+H). Anal. Calc. for $ZnC_{50}H_{32}N_2O_2$: C, 79.26; N, 3.70; H, 4.23. Found: C, 79.23; N, 3.81; H, 4.29%.

5.5. Devices fabrication

The ITO-coated glass substrate was first immersed sequentially in ultrasonic baths of acetone, alcohol and deionized water for 10 min, respectively, and then dried in an oven. The resistance of a sheet ITO is 50 Ω/□. The devices were fabricated in a multi-source organic molecule gas deposition system. There are different materials in every source, and the temperature of each source can be controlled independently. Different organic materials were deposited on the ITO-coated glass substrate according to the designed structure, LiF buffer layer and Al were deposited as a co-cathode under a pressure of 5×10^{-4} Pa. Electroluminescent spectra and commission international De L' Eclairage (CIE) coordination of these devices were measured by a PR655 spectra scan spectrometer. The luminescent brightness (L)–current (I)–voltage (V) characteristics were recorded simultaneously with the measurement of the EL spectra by combining the spectrometer through a Keithly model 2400 programmable voltage-current source. The current efficiency (E) was decided by this formula, $E = Ls/I$, then the power efficiency (η_P) was calculated by formula of $\eta_P = \pi L/IV$, where L is the luminescent brightness, s is the luminescent area, I is the current, and V is the voltage. The layer thicknesses of the deposited materials were monitored in situ using a model FTM-V oscillating quartz thickness monitor made in Shanghai, China. All the measurements were carried out at room temperature under ambient conditions.

Acknowledgements

Financial support from the National Natural Science Foundation of China (Nos. 20671036, 2007A010500008 and 2008B010800030) are gratefully acknowledged. Ouyang X H would like to acknowledge the receipt of the Doctorate Foundation from South China University of Technology (SCUT), Guangzhou and the China Scholarship Council. J.L. is a Cheung Kong Guest Chair Professor associated with SCUT.

Appendix A. Supplementary material

Supplementary data associated with this article can be found, in the online version, at doi:10.1016/j.jorganchem.2009.06.022.

References

[1] J.L. Garcia-Alvarez, Curr. Org. Chem. 12 (2008) 1199.
[2] S.C. Jain, A.K. Kapoor, W. Geens, J. Poortmans, R. Mertens, M.J. Willander, Appl. Phys. 92 (2002) 3752.
[3] A.E.W. Sarhan, Y. Nouchi, T. Izumi, Tetrahedron 59 (2003) 6353.
[4] V.K. Rai, R. Srivastava, M.N. Kamalasanan, Synthetic Met. 159 (2009) 234.
[5] N. Matsumoto, T. Miyazaki, M. Nishiyama, C.J. Adachi, Phys. Chem. C 113 (2009) 6261.
[6] Z.W. Liu, Z.Q. Bian, F. Hao, D.B. Nie, F. Ding, Z.Q. Chen, C.H. Huang, Org. Electron. 10 (2009) 247.
[7] Y.T. Tao, Q. Wang, Y. Shang, C.L. Yang, L. Ao, J.G. Qin, D.G. Ma, Z.G. Shuai, Chem. Commun. (2009) 77.
[8] C.H. Chang, Y.J. Lu, C.C. Liu, Y.H. Yeh, C.C.J. Wu, Disp. Technol. 3 (2007) 193–199.
[9] A. Liedtke, M. O'Neill, A. Wertmoller, S.P. Kitney, S.M. Kelly, Chem. Mater. 20 (2008) 3579.
[10] M.C. Gather, R. Alle, H. Becker, K. Meerholz, Adv. Mater. 19 (2007) 4460.
[11] C.W. Tang, S.A. VanSlyke, Appl. Phys. Lett. 51 (1987) 913.
[12] A. Mishra, P.K. Nayak, N. Periasamy, Tetrahedron Lett. 45 (2004) 6265.
[13] Z. Cui, S.H. Kim, Chinese Sci. Bull. 49 (2004) 797.
[14] J. Xie, Z. Ning, H. Tian, Tetrahedron Lett. 46 (2005) 8559.
[15] H.P. Zhao, X.T. Tao, P. Wang, Y. Ren, J.X. Yang, Y.X. Yan, C.X. Yuan, H.J. Liu, D.C. Zou, M.H. Jiang, A. Jiang, Org. Electron. 8 (2007) 673.
[16] H.P. Zhao, X.T. Tao, F.Z. Wang, Y. Ren, X.Q. Sun, J.X. Yang, Y.X. Yan, D.C. Zou, X. Zhao, M.H. Jiang, Chem. Phys. Lett. 439 (2007) 132.
[17] J. Jo, D. Vak, Y.Y. Noh, S.S. Kim, B. Lim, D.Y. Kim, J. Mater. Chem. 18 (2008) 654.
[18] H. Suh, Y. Jin, S.H. Park, D. Kim, J. Kim, C. Kim, J.Y. Kim, K. Lee, Macromolecules 38 (2005) 6285.
[19] İ. Kaya, A. Çetìner, M.J. Saçak, Maromol. Sci. A 44 (2007) 463.
[20] M.A. Noginov, M. Vondrova, S.N. Wiliams, M. Bahoura, V.I. Gavrilenko, S.M. Black, V.P. Drachev, V.M. Shalaev, A.J. Sykes, Opt. A-Pure Appl. Op. 7 (2005) s219.
[21] H. Cao, Z. Chen, Y. Liu, B. Qu, S. Xu, S. Cao, Z. Lan, Z. Wang, Q. Gong, Synthetic Met. 157 (2007) 427.
[22] T.H. Lee, K.L. Tong, S.K. So, L.M. Leung, Synthetic Met. 155 (2005) 116.
[23] M.G. Hutchings, I. Ferguson, S. Allen, J.E. Shearman, MCLC S&T B Nonlinear. Opt. 7 (1994) 157.